Songklanakarin J. Sci. Technol.
41 (5), 1184-1191, Sep. – Oct. 2019

http://www.sjst.psu.ac.th

Original Article

Comparative evaluation of thermal properties, tensile strain capacity and thermal cracking of concrete containing fly ash and slag

Arosha Dabarera[1], Warangkana Saengsoy[1*], Krittiya Kaewmanee[1], Takeshi Nakazaki[2], Thanapatch Lerdsupavaree[3], and Somnuk Tangtermsirikul[3]

[1] *Construction and Maintenance Technology Research Center, School of Civil Engineering and Technology, Sirindhorn International Institute of Technology, Thammasat University, Khlong Luang, Pathum Thani, 12120 Thailand*

[2] *Department of Research and Development II, Central Research Laboratory, Taiheiyo Cement Corporation, Chiba Prefecture, 285-8655 Japan*

[3] *School of Civil Engineering and Technology, Sirindhorn International Institute of Technology, Thammasat University, Khlong Luang, Pathum Thani, 12120 Thailand*

Received: 4 April 2018; Revised: 6 June 2018; Accepted: 21 June 2018

Abstract

Fly ash and slag are two SCM's utilized widely as partial replacements of cement in mass concrete. Different chemical, physical properties and reaction behavior cause fly ash-cement blend to differ from slag-cement blend in terms of thermal properties and thermal cracking in mass concrete. In this study, the time-dependent behavior of specific heat, thermal conductivity, and coefficient of thermal expansion (CTE) of hardening cement pastes containing fly ash and slag are comparatively investigated. Time-dependent models are proposed with satisfactory fit to the test results. A detailed comparison is done using finite element analysis of a mass concrete sample to evaluate thermal cracking potential, by comparing the predicted maximum restrained strain to the tested tensile strain capacity. The results indicate that fly ash performs better with lesser thermal cracking potential than slag in concrete mixes designed for similar long-term strengths.

Keywords: fly ash, mass concrete, slag, thermal cracking, thermal properties

1. Introduction

Evaluating the thermal behavior is essential in investigating and/or mitigating thermal cracking potential, especially at an early age of mass concrete structures. The heat generated by the exothermic hydration of cement dissipates rapidly in concrete members of relatively small dimensions. However, in mass concrete, the accumulated heat inside causes heat conduction with a thermal gradient along the cross section from center towards surface (Saengsoy & Tangtermsirikul, 2003). This temperature gradient causes thermal cracking if the induced restrained strain exceeds the tensile strain capacity of the mass concrete structure (Lu, Swaddiwudhipong, & Wee, 2001; Tongaroonsri & Tangtermsirikul, 2008). Thermal cracking has negative effects, such as reducing the integrity of concrete, accelerating corrosion of reinforcing bars, and reducing the service life of the structure.

Supplementary Cementitious Materials (SCM's) are used to reduce the rate of heat generation in mass concrete structures (Wang & Linger, 2010). Fly ash and slag are two key SCM's utilized as partial replacements of cement, due to their lower reactivity and heat generation at an early age. Fly ash is a pozzolanic material from coal combustion in thermal power plants. Ground Granulated Blast Furnace Slag (here referred to simply as slag) is a SCM obtained as a by-product

*Corresponding author
Email address: warangkana@siit.tu.ac.th

from steel manufacturing, and it shows both latent hydraulic and pozzolanic characteristics (Kolani *et al.*, 2012). It is evident that different chemical and physical properties and reaction behaviors cause fly ash-cement blend to differ from slag-cement blend in concrete.

The thermal properties, such as specific heat, thermal conductivity, and coefficient of thermal expansion (CTE) are required for accurate estimates of thermal cracking risk in mass concrete. Specific heat represents the heat capacity of concrete and is affected by the hydration of binders. It is a time-dependent property and changes rapidly in the early stages after casting of concrete, due to the reduction of free water content (Choktaweekarn, Saengsoy, & Tangtermsirikul, 2009a). Thermal conductivity (k) is important in heat transfer analysis of early stages of mass concrete structures. The phase composition change due to hydration can alter the conductivity of concrete, especially in the early stages (Choktaweekarn, Saengsoy, & Tangtermsirikul, 2009b). CTE is one of the major properties used on estimating the the thermal strains induced by temperature gradient in mass concrete.

Tensile strain capacity (TSC) is the maximum strain that concrete can sustain in tension prior to the first crack occurrence (Tongaroonsri & Tangtermsirikul, 2008). TSC has been used as a criterion in evaluation of thermal cracking risks in mass concrete structures (Choktaweekarn & Tangtermsirikul, 2010). Wee, Lu and Swaddiwudhipong (2000) tested TSC using direct tension test and flexural strength test methods. The TSC of concrete was between 150 με and 210 με in flexural strength test, and between 100 με and 140 με in direct tension test. Tongaroonsri and Tangtermsirikul (2008) investigated TSC using flexural strength method in order to find the effects of different mix proportions on the TSC of concrete. It was concluded that different binder compositions changed the interfacial transition zone (ITZ) properties, thereby affecting the TSC of concrete. Weaker ITZ leads to lower TSC since cracks most likely penetrate via ITZ rather than through strong aggregates or paste far from the ITZ.

In this study, specific heat, thermal conductivity, and CTE of cement pastes containing fly ash and slag are experimentally investigated, and time-dependent models of them are developed. TSC of the two concrete mixes, containing fly ash or slag, with similar long-term strengths is tested. This is followed by a finite element analysis of these two mass concrete mixes, containing fly ash or slag, simulating semi-adiabatic temperature and restrained strain profiles. Evaluation of thermal cracking risk is carried out by comparing the tested TSC values with the numerical estimates of maximum restrained strain.

2. Methodology

2.1 Experimental procedure

Specific heat and thermal conductivity measurements of hardening cement pastes were obtained by a method based on transiently heated plane sensor, using the instrument named Hot Disk Thermal Constants Analyser. During the test, a constant current is supplied to the sensor that is fitted between two pieces of a specimen to provide a slight temperature increment. The sensor serves both as a resistance and a temperature monitoring device, recording a time profile. Theory of this method has been summarized in prior studies (Bentz, 2007; He, 2005; Log & Gustafsson, 1995). CTE of each hardening cement paste was obtained by measuring length change of the specimen when subjected to a temperature change, and this method was previously used by Choktaweekarn and Tangtermsirikul (2009). It is reported that the magnitude of CTE does not vary in the normal range of temperatures, including those in mass concrete (Choktaweekarn & Tangtermsirikul, 2009; Klieger & Lamond, 1994). Therefore, temperatures between 30°C and 10°C were used in this study. Changes in temperature are observed using a thermocouple embedded at the center of each specimen.

A total of eight mixtures were cast to test specific heat, thermal conductivity, and CTE of paste specimens containing different levels of slag replacement. Water to binder ratio (w/b) of 0.40 was used. Slag replacements of 0%, 45%, 60%, and 75% were tested. Test results of pastes containing fly ash with different replacement levels were obtained from previous studies (Choktaweekarn *et al.*, 2009a, 2009b; Choktaweekarn & Tangtermsirikul, 2009) for comparison purposes. Mixes with w/b of 0.40 and fly ash replacements of 0%, 30% and 50% were used in the previous studies. Mixture labels have S or R for slag or fly ash replacements, respectively. For example, "W40 S45" indicates a paste mixture having w/b of 0.40 and slag replacement of 45%. The curing conditions of the specimens are such that there is no moisture loss or gain, in order to have similar conditions as inside mass concrete structures. The tests were carried out at 3, 7, and 28 days after casting of paste samples.

TSC of concrete can be measured using either direct tension test or flexural test. However, TSC evaluated using flexural test was selected due to the non-uniform stress distribution along the cross section, which is similar to the stress distribution in real mass concrete structures. Therefore, the third point loading test method (ASTM C 78) was used to determine the cracking strain of the concrete mixes.

Two concrete mixes containing 50% fly ash (50FA) and 65% slag (65Slag) with an equivalent strength of 30MPa at 56 days were tested for TSC. Trial mixes were tested to obtain similar compressive strengths at 56 days. Prismatic beams with dimensions of 100×100×350mm were cast, demoulded after 1 day, and kept in water curing condition until tested. The tests were carried out at 1, 3, 7, and 28 days after casting. Prior to the test, three displacement transducers were attached to the tensile surface within the constant moment span of each specimen. The first crack occurrence was detected using a conductive pencil line drawn on the tensile surface of the beam, connected to a 9 volt battery and data logger. The crack detection technique using a pencil line in circuit was adopted from prior studies (Tongaroonsri & Tangtermsirikul, 2008; Wang & Zheng, 2005).

The binders used in this study are Ordinary Portland Cement (OPC), slag, and fly ash. The chemical compositions and physical properties of the binders are shown in Table 1. The mix proportions of the concrete mixes (50FA & 65 Slag) used for FEM analysis and TSC tests are shown in Table 2.

2.2 Simulation of thermal cracking

Shown in Figure 1 is a flowchart demonstrating a step by step procedure to evaluate the thermal cracking potential. Having the heat of hydration of binders as described in our previous studies (Dabarera, Saengsoy, Kaewmanee, Mori, & Tangtermsirikul, 2017; Saengsoy & Tangtermsirikul, 2003; Tangtermsirikul & Saengsoy, 2002), specific heat, and thermal conductivity as inputs, semi-adiabatic temperature distribution can be derived from heat transfer analysis using finite element method. Then, with the computed CTE, a stress analysis is carried out to obtain restrained strains due to differential thermal deformations. Then, the maximum restrained strains from the finite element analysis are compared with measured tensile strain capacity of the concrete, in order to evaluate the thermal cracking potential in this study.

Two concrete mixes containing 50% fly ash or 65% slag replacements, which were designed for strength of 30MPa at 56 days, were selected for this case study. A finite element analysis was carried out using a commercial FEM program (MARC). In this paper, semi-adiabatic temperature and restrained strain of a mass concrete sample with dimensions 26×26×3 m were investigated. The top, mid depth, and bottom points at center, x-rim and y-rim were considered as the analysis points for this study, and their locations are shown in Figure 2. In order to simulate mass concrete environment, the sample was insulated with 3 inches thick

Table 1. Chemical compositions and physical properties of Ordinary Portland Cement type I, slag, and fly ash.

Binder	Chemical compositions [% by weight]						Blaine's fineness [cm^2/g]	Specific gravity [g/cm^3]	Ignition loss[%]
	SiO_2	Al_2O_3	Fe_2O_3	CaO	MgO	SO_3			
OPC	22.0	5.40	3.0	63.4	2.7	2.0	3570	3.16	2.40
Slag	33.5	14.35	0.26	43.3	5.1	2.1	4330	2.89	0.96
Fly ash	36.1	19.4	15.1	17.4	3.0	0.8	2510	2.10	2.81

Table 2. Mix proportions of the concrete mixes with 50% FA and 65% slag.

Mix	Total binder (kg/m^3)	w/b	Cement (kg/m^3)	Fly ash (kg/m^3)	Slag (kg/m^3)	Water (kg/m^3)	Sand (kg/m^3)	Gravel (kg/m^3)
50%FA	324	0.46	162	162	-	149	835	1076
65% Slag	323	0.60	113	-	210	194	799	1029

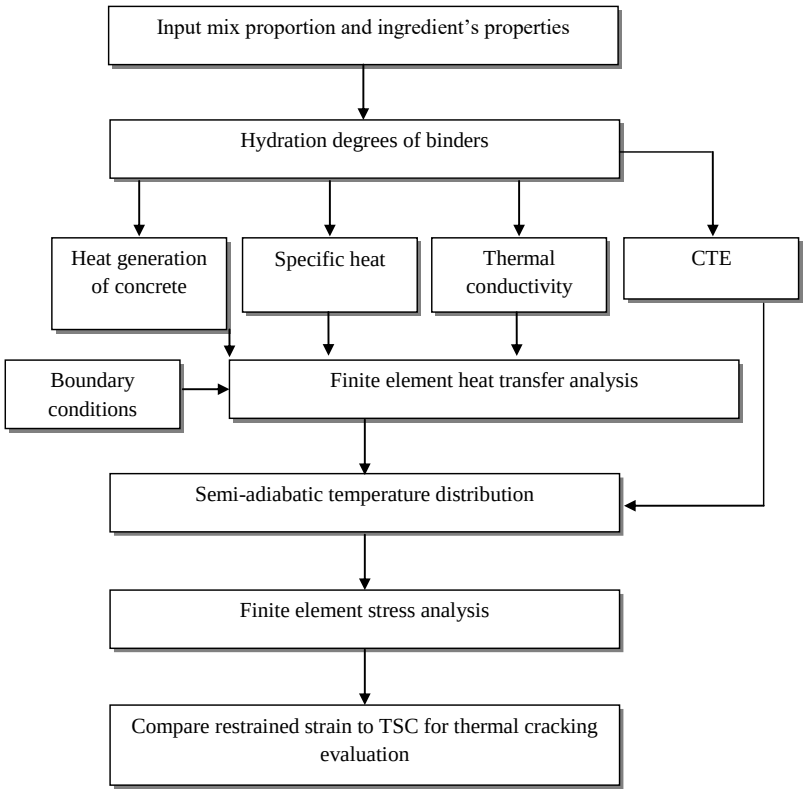

Figure 1. Flow chart for thermal cracking risk assessment of mass concrete.

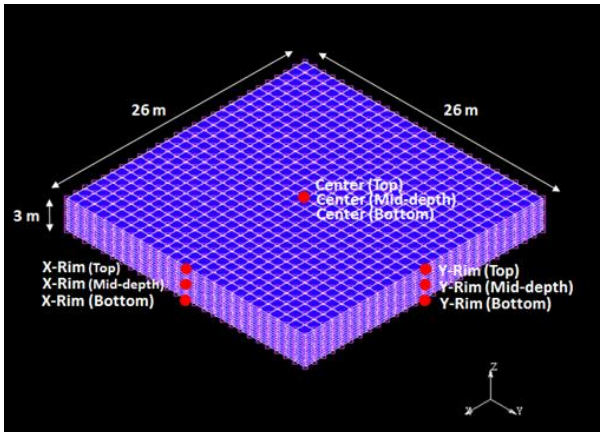

Figure 2. Finite elements mesh and analyzed points.

foam at all surfaces. Steel formwork with 1 cm thickness and an ambient temperature of 32°C were assumed for this analysis. The semi-adiabatic temperature distribution and maximum restrained strain were obtained and compared with the Tensile Strain Capacities (TSC's) to evaluate the thermal cracking potential of the two concrete mixes, 50% fly ash replacement and 65% slag replacement.

Two concrete mixes containing 50% fly ash or 65% slag replacements, which were designed for strength of 30MPa at 56 days, were selected for this case study. A finite element analysis was carried out using a commercial FEM program (MARC). In this paper, semi-adiabatic temperature and restrained strain of a mass concrete sample with dimensions 26×26×3 m were investigated. The top, mid depth, and bottom points at center, x-rim and y-rim were considered as the analysis points for this study, and their locations are shown in Figure 2. In order to simulate mass concrete environment, the sample was insulated with 3 inches thick foam at all surfaces. Steel formwork with 1 cm thickness and an ambient temperature of 32°C were assumed for this analysis. The semi-adiabatic temperature distribution and maximum restrained strain were obtained and compared with the Tensile Strain Capacities (TSC's) to evaluate the thermal cracking potential of the two concrete mixes, 50% fly ash replacement and 65% slag replacement.

3. Specific Heat

3.1 Experimental results

Figure 3 shows the test results of specific heat of pastes containing slag and fly ash for up to 28 days. It is observed that the specific heat is a time-dependent property, which significantly decreases with time regardless of the SCM utilized. This is due to decreased amount of free water with time (Tangtermsirikul & Saengsoy, 2002). The specific heats of pastes containing fly ash are slightly higher than of those containing slag, especially at an early age. This is considered to be due to self-hydrating ability of the slag at an early age, which consumes more free water than the purely pozzolanic reactions of fly ash (Dabarera *et al.*, 2017). However, the rate of change of specific heat in a longer term is higher in the pastes containing fly ash than in those with slag, due to later age pozzolanic reactions of fly ash.

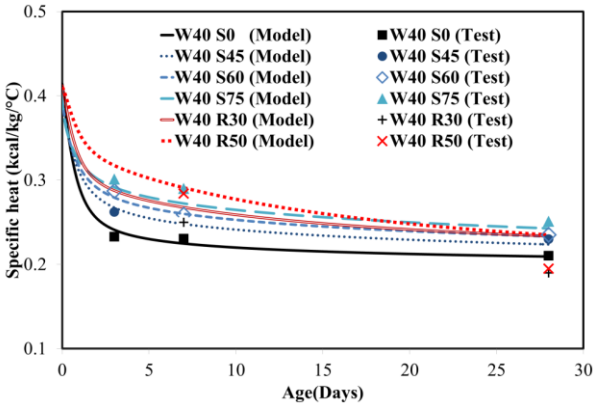

Figure 3. Comparison of tested and predicted specific heats of pastes with 0%, 45%, 60%, and 75% slag and with 30%, 50% fly ash, at w/b=0.40.

3.2 Model for predicting specific heat capacity

A time-dependent model for the specific heat of pastes, mortars and concrete was developed by Choktaweekarn *et al.* (2009a). Using this model, the specific heat of concrete at a given time can be calculated based on weight fraction of each constituent and their specific heats. This model was further extended by Dabarera *et al.* (2017) so it takes into account the effects of slag. The equation for computing time-dependent specific heat of concrete is shown in Equation 1.

$$c(t) = w_g c_g + w_s c_s + w_{fw}(t)c_w + w_{uc}(t)c_c + w_{ui}(t)c_i + w_{hp,i}(t)c_{hp,i} \quad (1)$$

Here c(t) is the specific heat of concrete at the considered age t (kcal/kg/°C). w_g and w_s are the weight ratios of coarse and fine aggregates per unit weight of concrete, respectively. $w_{fw}(t)$, $w_{uc}(t)$, $w_{ui}(t)$ and $w_{hp,i}(t)$ are the weight ratios of free water, un-hydrated cement, non-reacted slag or non-reacted fly ash, and the hydrated products of slag concrete or fly ash concrete, respectively, at the considered age t. These parameters are computed based on hydration degrees of the binders (Dabarera *et al.*, 2017; Saengsoy & Tangtermsirikul, 2003; Tangtermsirikul & Saengsoy, 2002). The term i denotes the SCM which is used to replace cement partially, in this study either slag or fly ash. c_g, c_s, c_w, c_c, c_i, and $c_{hp,i}$ are specific heat values of coarse aggregate, fine aggregate, water, cement, slag or fly ash, and hydrated products, respectively (kcal/kg/°C). The values were obtained from our previous studies (Choktaweekarn *et al.*, 2009a ; Dabarera *et al.*, 2017). The model predictions for pastes containing slag and fly ash are shown by lines in Figure 3. The model simulations matched the test results with a reasonable accuracy.

4. Thermal Conductivity

4.1 Experimental results

Figure 4 shows the measured thermal conductivities of pastes containing slag and fly ash for up to 28 days. The results indicate slight increase in thermal conductivity with

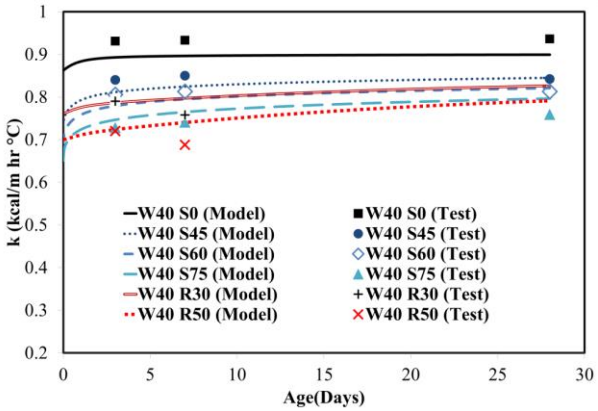

Figure 4. Comparison of tested and predicted thermal conductivity for pastes with 0%, 45%, 60%, and 75% slag and with 30%, 50% fly ash, at w/b=0.40.

time, due to increased hydrated products and continuity of paste structure.

The thermal conductivities of pastes containing slag and fly ash replacements are lower than that of cement paste. Lower replacements of fly ash utilized in this study show a considerably decreased thermal conductivity relative to cases with high slag replacements. This is expected to be due to discontinuity of the paste structure and lower density of the pastes containing fly ash than of those with slag. Similar observations were reported by Demirboga (2007) and Damdelen, Georgopoulos and Limbachiya (2014).

4.2 Model for predicting thermal conductivity

A time-dependent model which computes thermal conductivity of fly ash concrete was developed by Choktaweekarn *et al.* (2009b). In this model, thermal conductivity of concrete at a given time can be calculated based on volume fraction and thermal conductivity of each constituent of concrete. Model for slag concrete was also proposed based on similar concepts as in our previous study (Dabarera *et al.*, 2017). The equation for computing time-dependent thermal conductivity of concrete is shown in Equation 2.

$$k(t) = n_g k_g + n_s k_s + n_{fw}(t)k_w + n_{uc}(t)k_c + n_{ui}(t)k_i + n_{hp,i}(t)k_{hp,i} \quad (2)$$

Here k(t) is thermal conductivity of concrete at the considered age (kcal/m hr °C), k_g, k_s, k_w, k_c, k_i, k_{ra}, $k_{hp,i}$ are thermal conductivities of coarse aggregate, fine aggregate, free water, cement, slag or fly ash, air and hydrated products, respectively. The values were summarized in previous studies (Choktaweekarn *et al.*, 2009b: Dabarera *et al.*, 2017). The term i denotes the SCM which is used to replace cement partially, in this study either slag or fly ash. n_g, n_s , and n_{ra}, are volumetric ratios of coarse aggregate, fine aggregate and air, respectively. $n_{fw}(t)$, $n_{uc}(t)$, $n_{ui}(t)$ and $n_{hp,i}(t)$ are volumetric ratios of free water, un-hydrated cement, non-reacted slag or fly ash and hydrated product at the considered age, which are computed based on hydration degrees of the binders. The model predictions for pastes containing slag and fly ash are shown by lines in Figure 4. The model simulations predicted the test results with a reasonable accuracy.

5. Coefficient of Thermal Expansion (CTE)

5.1 Experimental results

Figure 5 shows the test results of CTE of pastes containing fly ash and slag, for up to 28 days. The results show that the CTE of paste is time-dependent and increases with time due to increase of continuity of the paste structure. From the test results in Figure 5, it is observed that the CTE of pastes containing slag and fly ash are lower than that of the cement paste. This is due to the lower CTE of these SCM's when compared to that of cement. Pastes containing fly ash show significant decrease of CTE when compared to that of slag, especially at an early age. This is due to the lower continuity of the paste structure and lower CTE of the pastes containing fly ash when compared to that of slag. However, the difference in CTE becomes less and the CTE values increase due to activation of pozzolanic reactions of both fly ash and slag at a later age.

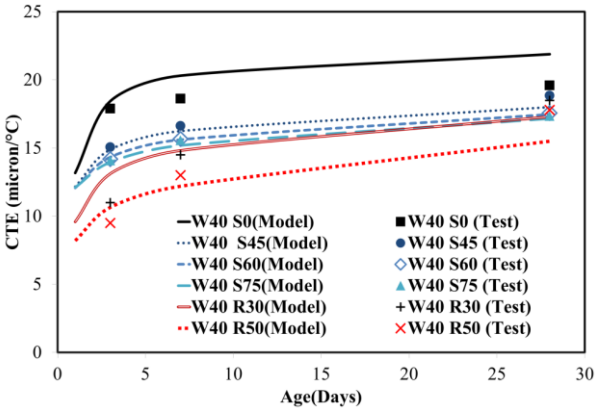

Figure 5. Comparison of tested and predicted CTE values of pastes with 0%, 45%, 60%, and 75% slag and 30%, 50% fly ash at w/b=0.40.

5.2 Model for predicting CTE

Aggregates govern the CTE of concrete since most of it by volume is aggregates. A time-dependent model which computes CTE of concrete containing fly ash was developed in a previous study by our research group (Choktaweekarn & Tangtermsirikul, 2009). The model is a function of volumetric fraction, modulus of elasticity, and CTE of each ingredient in concrete, as shown in Equation 3.

$$CTE(t) = \frac{(n_p CTE_p(t) E_p(t) + n_s CTE_s E_s + n_g CTE_g E_g)}{(n_p E_p(t) + n_s E_s + n_g E_g)} \quad (3)$$

Here CTE(t) is the CTE of mortar or concrete at the considered age (microns/°C), CTE_p, CTE_s and CTE_g are the CTE of paste, sand and coarse aggregate, respectively (microns/°C). n_p, n_s and n_g are the volumetric ratios of paste, sand, and coarse aggregate, respectively. The modulus of elasticity of aggregate phase was obtained from Tangterm-sirikul and Tatong (2001). The modulus of elasticity of paste

was modeled as a time-dependent variable which depends on the compressive strength of the paste at the time considered.
The CTE of paste (CTE_p) is an important parameter affected by the time-dependent volume fractions of non-reacted cementitious materials and hydrated products. Thus, the CTE of cement paste at a given time is modeled based on volume fractions of non-reacted binder content and hydrated product amounts. The equation for computing time-dependent CTE of paste is shown in Equation 4.

$$CTE_p(t) = an_{p,uc}(t)CTE_c + bn_{p,ui}(t)CTE_i + cn_{p,hp,i}(t)CTE_{hp,i} \quad (4)$$

$CTE_p(t)$ is the CTE of paste at the considered age (microns/°C), CTE_c, CTE_i and $CTE_{hp,i}$ are the CTE of cement, slag or fly ash (denoted by the parameter i), and the hydrated products of cement pastes that have been previously summarized (Choktaweekarn & Tangtermsirikul, 2009; Dabarera *et al.*, 2017). $n_{p,uc}(t)$, $n_{p,ui}(t)$ and $n_{p,hp,i}(t)$ are the volumetric ratios of un-hydrated cement, non-reacted slag or fly ash and hydrated products of cement pastes at the considered age, which are computed based on hydration degrees of the binders. The constants a, b and c are derived by regression analysis from test results of pastes with different slag or fly ash replacements. The a, b, and c values for paste with fly ash and slag are 0.284, 1.23, 1.499 and 0.284, 2, 1.4, respectively. The model predictions for pastes containing slag and fly ash are shown by lines in Figure 5 where the test results are matched with a reasonable accuracy.

6. Thermal Cracking Evaluation Using Finite Element Analysis and Test Results

6.1 Semi-adiabatic temperature rise

The characteristics of the semi-adiabatic temperature profiles of the two analysed concrete mixes are summarized in Table 3. Peak temperatures of the concrete mixes with fly ash and slag are 61.5°C and 66°C, respectively. Thus, the fly ash concrete possesses lower peak temperature than the slag concrete. Moreover, time to attain peak temperature is delayed in the fly ash concrete when compared to the slag concrete, as shown in Table 3. This proves that the fly ash concrete analyzed in this study has notable benefits over the slag concrete in terms of minimizing temperature rise at an early age.

6.2 Tensile Strain Capacity (TSC) test results

The test results for TSC of 50FA and 65Slag concrete mixes at 1, 3, 7, and 28 days are shown in Figure 6. The TSC increased with age due to enhanced paste strength and quality of ITZ with time. The results clearly show that the cracking strains of 65Slag concrete mix are higher than those of the 50FA mix, especially at an early age. This is due to the ability of slag to attain high early age strength owing to its self-hydrating and pozzolanic characteristics (Dabarera *et al.*, 2017). However, TSC of 50FA gradually increases with time and almost reaches similar values with 65Slag mix at 28 days. This is due to the increase of the paste strength from the pozzolanic reaction of fly ash at a later age.

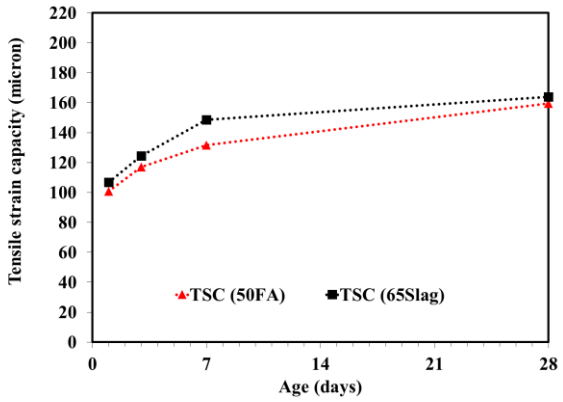

Figure 6. TSC test results of concrete with 50% fly ash and 65% slag.

6.3 Comparison of maximum restrained strain and TSC

The restrained strain was analyzed at different points of the mass concrete samples, shown in Figure 2. The temperature at each position in the mass concrete at each time step, obtained from the heat transfer analysis, was used as the input for restrained strain analysis. The centre portion of the analyzed sample is restrained from free thermal expansion so that compressive stress is induced, whereas tensile stress occurs near the surface to counter balance the compressive stress at the centre portion. Thus, the maximum restrained tensile strain at the top surface is used to explain the potential of thermal cracking.

Table 3. Characteristics of simulated semi-adiabatic temperature rise and thermal cracking potential of concrete with 50% fly ash or with 65% slag.

Characteristics of simulated semi-adiabatic temperature rise		
Mix	50FA	65Slag
Maximum temperature (°C)	61.5	66.0
Temperature rise (°C)	29.5	34.0
Time at peak temperature	5 days & 6 hours	3 days & 18 hours
Characteristics of thermal cracking potential evaluation		
Mix	50FA	65Slag
Maximum restrained strain ($\times 10^{-6}$)	137	158
Cracking age (hours)	27.2	20.4
Cracking strain ($\times 10^{-6}$)	102	104
$\Delta\varepsilon$ ($\times 10^{-6}$)	35 ($\Delta\varepsilon_{fa}$)	54($\Delta\varepsilon_{slag}$)

Thermal cracking occurs when the restrained strain exceeds the TSC at some location of the structure. In this paper, tests were carried out to obtain the TSC's of concrete with 50% fly ash and 65% slag. Then maximum restrained strain obtained from finite element analysis was plotted along with TSC test results of each mix in order to evaluate the thermal cracking risk.

Figure 7 (a) and 7 (b) show the maximum restrained strain and TSC of the fly ash concrete and the slag concrete, respectively. A comparison of characteristics in Figure 7 (a) and 7 (b) is shown in Table 3. The maximum restrained strains for fly ash concrete and slag concrete were 137 microns and 158 microns, respectively. It is seen that fly ash concrete had lesser maximum restrained strain at an early age when compared to the slag concrete.

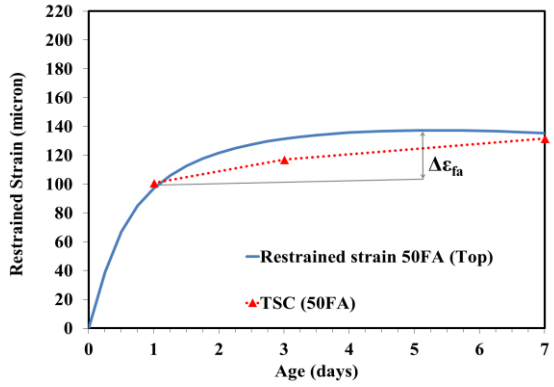

(a)

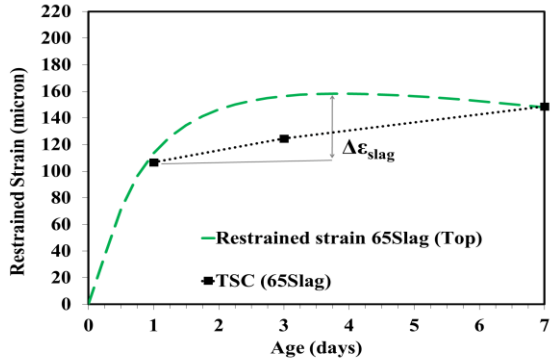

(b)

Figure 7. Comparison of TSC and predicted restrained strain of (a) concrete with 50% fly ash (b) concrete with 65% slag.

The point where restrained strain reaches TSC was considered as the first thermal cracking occurrence point. Cracking is expected to occur at 27.2 and 20.4 hours after casting in fly ash concrete and slag concrete, respectively. The strain at cracking is slightly higher in slag concrete than in fly ash concrete. Moreover, it can be observed that the difference between maximum restrained strain and TSC of the slag concrete ($\Delta\varepsilon_{slag}$) is higher than that of the fly ash concrete ($\Delta\varepsilon_{fa}$). This indicates potentially lower crack width in the fly ash concrete and then likely less reinforcement is required for crack width control than would be required in slag concrete. This comparison shows that the fly ash concrete analyzed in this paper performs better than the slag concrete, and minimizes thermal cracking potential in the analyzed mass concrete structure.

7. Conclusions

In this study, the time-dependent behaviors of specific heat, thermal conductivity, and coefficient of thermal expansion (CTE) of cement pastes containing fly ash or slag were comparatively investigated, and time-dependent models were proposed. Then, these models were used as inputs along with heat of hydration of binders from the author's previous studies, to investigate thermal cracking potential of two concrete mixes, containing 50% fly ash or 65% slag, having equal compressive strengths at 56 days. The thermal cracking analysis showed that the fly ash concrete analyzed in this paper performs better than the slag concrete, minimizing thermal cracking potential of the analyzed mass concrete structure.

Acknowledgements

The authors would like to acknowledge the Centre of Excellence in Material Science, Construction and Maintenance Technology, Thammasat University, Thailand and Taiheiyo Cement Corporation, Japan for the support and funding for this project.

References

Bentz, D. (2007). Transient plane source measurements of the thermal properties of hydrating cement pastes. *Materials and Structures, 40*(1), 1073-1080.

Choktaweekarn, P., & Tangtermsirikul, S. (2009). A model for predicting the coefficient of thermal expansion of cementitious pastes. *Science Asia, 35*(2), 57-63.

Choktaweekarn, P., & Tangtermsirikul, S. (2010). Effect of aggregate type, casting, thickness and curing condition on restrained strain of mass concrete. *Songklanakarin Journal of Science and Technology, 32*(4), 391-402.

Choktaweekarn, P., Saengsoy, W., & Tangtermsirikul, S. (2009). A model for predicting specific heat capacity of fly-ash concrete. *Science Asia, 35*(2), 178-182.

Choktaweekarn, P., Saengsoy, W., & Tangtermsirikul, S. (2009). A model for predicting thermal conducivity of concrete. *Magazine of Concrete Research, 61*(4), 271-280.

Dabarera, A., Saengsoy, W., Kaewmanee, K., Mori, K., & Tangtermsirikul, S. (2017). Models for predicting hydration degree and adiabatic temperature rise of mass concrete containing ground granulated blast furnace slag. *Engineering Journal, 21*(3), 157-171.

Damdelen, O., Georgopoulos, C., & Limbachiya, M. (2014). Measuring Thermal mass in sustainable concrete mixes. *Journal of Civil Engineering and Architecture Research, 1*(1), 60-70.

Demirboga, R. (2007). thermal conductivity and compressive strength of concrete incorporation with mineral admixtures. *Building and Environment, 42*, 2467-2471.

He, Y. (2005). Rapid thermal conductivity measurement with a hot disk sensor part 1. theoretical considerations. *Thermochimica Acta, 436*, 122-129.

Klieger, P., & Lamond, J. (1994). *Significance of Tests and Properties of Concrete and Concrete-Making Materials* (4th ed.). West Conshohocken, PA: ASTM International.

Kolani, B., Buffo-Lacarriere, L., Sellier, A., Escadeillas, G., Boutillon, L., & Linger, L. (2012). Hydration of Slag-blended cements. *Cement and Concrete Composites, 34*(1), 1009-1018.

Log, T., & Gustafsson, S. (1995). Transient Plane Source (TPS) technique for measuring thermal transport properties of building materials. *Fire Mater, 19*, 43-49.

Lu, H., Swaddiwudhipong, S., & Wee, T. (2001). Evaluation of thermal crack by a probabilistic model using the tensile strain capacity. *Magazine of Concrete Research, 53*(1), 28-30.

Saengsoy, W., & Tangtermsirikul, S. (2003). Model for predicting temperature of mass concrete. *Proceeding of the 4th Regional Symposium on Infrastructure Development in Civil Engineering (RSID4). Bangkok, Thailand.*

Tangtermsirikul, S., & Saengsoy, W. (2002). Simulation of free water content of paste with fly ash. *Research and Development Journal of the Engineering Institute of Thailand, 13*(4), 1-10.

Tangtermsirikul, S., & Tatong, S. (2001). Modeling of aggregate stiffness and its effect on shrinkage of concrete. *Science Asia, 27*(3), 185-192.

Tongaroonsri, S., & Tangtermsirikul, S. (2008). Influence of mixture condition and moisture on tensile strain capacity of concrete. *Science Asia, 34*(1), 59-68.

Wang, G., & Zheng, J. (2005). The influence of cementitious systems to cracking sensitivity of self-compacting concrete. *Proceeding of the 1st International Symposium on Design, Performance and Use of Self-Consolidating Concrete* (pp. 457-464), Changsha, China.

Wang, X., & Linger, H. (2010). Modelling the hydration of concrete incorporating fly ash or slag. *Cement and Concrete Research, 40*(1), 984-996.

Wee, T., Lu, H., & Swaddiwudhipong, S. (2000). Tensile strain capacity of concrete under various states of stress. *Magazine of Concrete Research*, 185-193.